Assessment of an LPG mPOF for Strain Sensing

Gaizka Durana, Javier Gómez, Gotzon Aldabaldetreku, Joseba Zubia, Ander Montero, and Idurre Sáez de Ocáriz

***Abstract*— We demonstrate the feasibility of long-period gratings (LPGs) written in microstructured polymer optical fibers (mPOFs) for detecting and measuring the strain rate and magnitude of engineering structures. We validate and compare the results of our experimental tests to a commercial fiber Bragg grating sensor. The encouraging results open the way to the use of LPG mPOF sensors in structural health monitoring applications.**

***Index Terms*— Microstructured optical fibers, plastic optical fibers (POFs), strain sensing, structural health monitoring.**

I. Introduction

GREAT research and development effort has been made in the field of optical fiber sensors during the last 15 years. This is due to the attractive properties of optical fibers such as electromagnetic interference immunity, being intrinsically safe, lightweight and able to provide continuous real-time analysis [1], [2]. More specifically, structural health monitoring (SHM) has attracted significant attention in a variety of disciplines including aerospace, civil, military and marine [3]. SHM is aimed at monitoring the damage caused to structures and their evolution by means of structurally-integrated sensors in order to get an early warning and avoid the structure to collapse.

To date, several optical fiber sensors have been proposed for SHM applications. Some of the most prominent solutions for SHM include intensity-based and interferometry-based optical fiber sensors, and fiber Bragg gratings [4]–[7]. The former, intensity-based sensors, represent one of the most direct and basic solutions used for SHM applications [8], [9]. These types of sensors rely on monitoring the signal intensity which is modulated in response to the measured quantity. Although intensity-based sensors suffer drawbacks such as intensity fluctuations of the light source or long-term intensity drifts, in applications where precise intensity level is not required they offer excellent performance monitoring oscillatory response under dynamic loading conditions [10]. The latter, fiber Bragg gratings (FBGs), which are commonly UV written in conventional single-mode silica fibers, have recently been demonstrated in polymer optical fibers (POFs) [11]–[15]. Some of those POF-based FBG sensors offer ease of handling, higher strain sensitivity and higher strain limit than silica-based FBGs. Although further research is required to improve and understand the grating writting process in POFs, the potential of POF-based FBG sensors for SHM applications is clear [16], [17].

Recently microstructured POFs (mPOFs) have attracted significant attention as a new type of fiber for sensing applications [18], [19]. A pattern of air holes running along the entire length of the fiber provides unique optical properties which may be tailored to a wide variety of sensing applications. Such optical properties include single-mode operation obtained from a single matrix material with guiding properties controlled by the photonic bandgap effect. Long period gratings (LPGs) have become an alternative to FBGs written in mPOFs as localized sensors. LPGs are easier to fabricate than Bragg gratings and the periodic structure is imprinted on the outer cladding of the mPOF. Therefore, LPGs written in single-mode mPOFs [20] offer an attractive approach to strain measurements [21]–[24].

In this paper, we demonstrate the suitability of LPG mPOFs for monitoring the strain level of a steel plate. For that purpose, we explain first the principles upon which the sensor is based. Afterwards, experimental details related to the preparation of the specimen and the experimental programme are explicated. Then, the most representative results are shown and discussed. Finally, the main conclusions drawn from the work are presented.

A. Sensor Principles

The mPOF used in the experimental programme is a single-mode microstructured design made of polymethyl methacrylate (PMMA) with a long period grating written in it [20]. The microstructure of the mPOF, depicted in Fig. 1(a), constains a hexagonal lattice of small holes defining the cladding region. The distance between holes is of $\Lambda = 5.15\,\mu$m, along with a hole diameter of $d = 2.80\,\mu$m. The size of the core is of $D = 7.0\,\mu$m with an external fiber diameter of 335 μm. LPGs are deterministic perturbations to the fiber which have been created using template imprinting upon a heated fiber [25], [26]. The transmission spectra of long period gratings show loss features at the resonant wavelengths where the core mode couples to a cladding mode. This wavelength is given by [25]

$$m\lambda = \left(n_{\mathbf{core}}(\lambda) - n^{i}_{\mathbf{cl}}(\lambda)\right)\Lambda_{\mathbf{LPG}} \tag{1}$$

where $\Lambda_{\mathbf{LPG}}$ is the pitch of the grating, m is the order of the interaction, and $n_{\mathbf{core}}$ and $n^{i}_{\mathbf{cl}}$ are, respectively, the effective indices of the core mode and the ith cladding mode. The wavelength of the loss feature depends strongly on the strain

Manuscript received December 9, 2011; revised February 29, 2012; accepted April 17, 2012. Date of publication May 15, 2012; date of current version June 13, 2012. The associate editor coordinating the review of this paper and approving it for publication was Dr. M. Nurul Abedin.

G. Durana, G. Aldabaldetreku, and J. Zubia are with the Department of Electronics and Telecommunications, University of the Basque Country, Bilbao E-48013, Spain (e-mail: gaizka.durana@ehu.es; gotzon.aldabaldetreku@ehu.es; joseba.zubia@ehu.es).

J. Gómez is with the University of the Basque Country, Bilbao E-48013, Spain (e-mail: javier.gomez@ehu.es).

A. Montero and I. Sáez de Ocáriz are with the Aeronautical Technologies Center, Vitoria 01510, Spain (e-mail: a.montero@ctaero.com).

Color versions of one or more of the figures in this paper are available online at http://ieeexplore.ieee.org.

Digital Object Identifier 10.1109/JSEN.2012.2199105

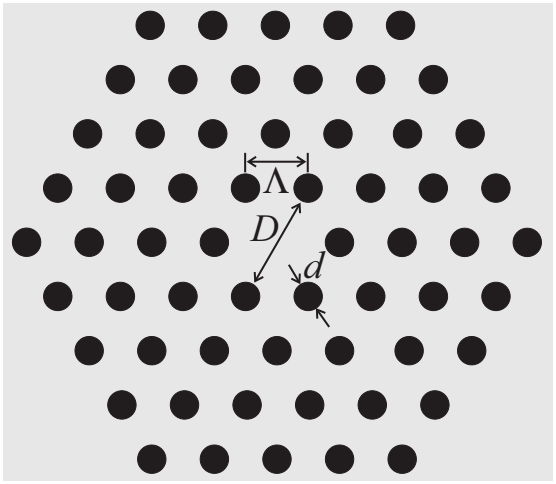

(a)

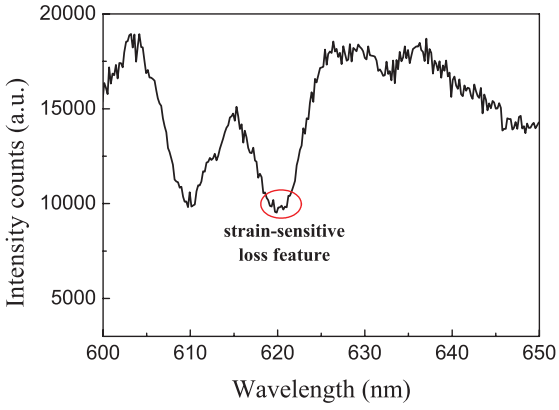

(b)

Fig. 1. Single-mode mPOF used in the experimental program. (a) Schematic representation of the microstructure showing the most important dimensions of the mPOF. (b) Transmission spectrum of one of the LPGs used in the tests. Loss feature wavelength corresponding to the strain-free case.

applied to the fiber. The amount of wavelength shift with axial strain ϵ is obtained by expanding Equation 1 and re-arranging to yield

$$\frac{d\lambda}{d\epsilon} = \frac{\partial\lambda}{\partial(\Delta n_{\mathbf{eff}})}\left(\frac{dn_{\mathbf{core}}}{d\epsilon} - \frac{dn^{i}_{\mathbf{cl}}}{d\epsilon}\right) + \Lambda_{\mathbf{LPG}}\frac{\partial\lambda}{\partial\Lambda_{\mathbf{LPG}}} \tag{2}$$

where $\Delta n_{\mathbf{eff}} = n_{\mathbf{core}} - n^{i}_{\mathbf{cl}}$, the dependence $\partial\lambda/\partial(\Delta n_{\mathrm{eff}})$ is obtained from differentiating Equation 1 and solving Λ_{LPG} from the obtained result, and we have used the definition of the dimensionless quantity $\Delta\epsilon = \Delta\Lambda/\Lambda$, i.e. $\partial\epsilon = \partial\Lambda_{\mathrm{LPG}}/\Lambda_{\mathrm{LPG}}$. Both terms on the right hand side of the equation are the contributions to the grating strain sensitivity due to the change in the differential effective index ($\Delta n_{\mathbf{eff}}$) and the grating periodicity ($\Lambda_{\mathbf{LPG}}$), usually referred to as the material and waveguide effects, respectively. The latter is usually the most significant effect and it is a function of the slope $\partial\lambda/\partial\Lambda_{\mathbf{LPG}}$ for a particular cladding mode, which can have either sign depending on the grating period [27]. In the case of the LPG used in this work, $\partial\lambda/\partial\Lambda_{\mathbf{LPG}}$ turns out to be negative so that any increase in the strain applied to the LPG implies a decrease in the resonant wavelength [20]. In contrast, in the case of

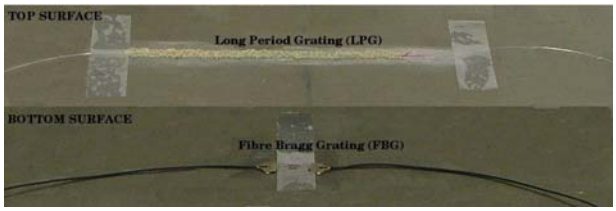

Fig. 2. Photograph showing the steel specimen with the LPG mPOF sensor (top surface) and the silica-based FBG sensor (bottom surface) fixed to it. The gauge length of the LPG was approximately 60 mm.

FBGs the amount of Bragg wavelength shift $\Delta\lambda_{\mathrm{B}}$ with axial strain ϵ is positive and given by [28]

$$\frac{\Delta\lambda_{\mathrm{B}}}{\lambda_{\mathrm{B}}} = (1 - p_{\mathrm{e}})\epsilon \tag{3}$$

where p_{e} is a coefficient dependent on the photoelastic coefficients of the grating material.

An example of a transmission spectrum of the LPG mPOF is shown in Fig. 1(b), where several loss features can be observed. Those are the result of the LPG imprinting process, which causes coupling from the core mode to different cladding modes. However, only the loss feature located at around 620 nm-wavelength is sensitive to strain.

Therefore, the sensing capability of the mPOF-based optical sensor relies on coupling white light into the fiber and on recording the change of the resonant wavelength λ with the strain applied to the fiber ϵ.

II. Experimental Details

A. Specimen Preparation

In this experimental programme we have considered two different scenarios to test the response of the sensor. In the first one, the long period grating was held between two rubber attachment clamps, with one of the ends fixed to a motorised linear stage of high precision. The rubber clamps were used to avoid fiber slippage. The linear stage applied uniform strain to the fiber in completely reproducible conditions. The loss feature was located at a wavelength of 596 nm with no applied strain, and the length of the mPOF was of 1 m.

In the second experimental scenario the LPG mPOF was surface-bonded to a rectangular steel plate of dimensions 1 m × 0.2 m × 0.01 m. After having tested different bonding materials, the most suitable solution consisted in applying a 2-part acrylic adhesive for plastics which does not require pre-treatment of the surface. However, we first polished the bonding surface with sandpaper, and then cleaned it with alcohol thoroughly before bonding the LPG all along its length to the surface. Figure 2 shows a picture of the steel proof specimen with the LPG surface bonded to it. A silica-based FBG was also attached to the opposite surface on the steel specimen as a reference. In this case, the FBG was fixed to the specimen following the instructions and bonding materials provided by the fiber manufacturer. Regarding the fiber location, both the mPOF and the FBG were fixed longitudinally at the centre of the specimen, the mPOF on one side and the FBG on the other side of the plate. The loss feature of the mPOF

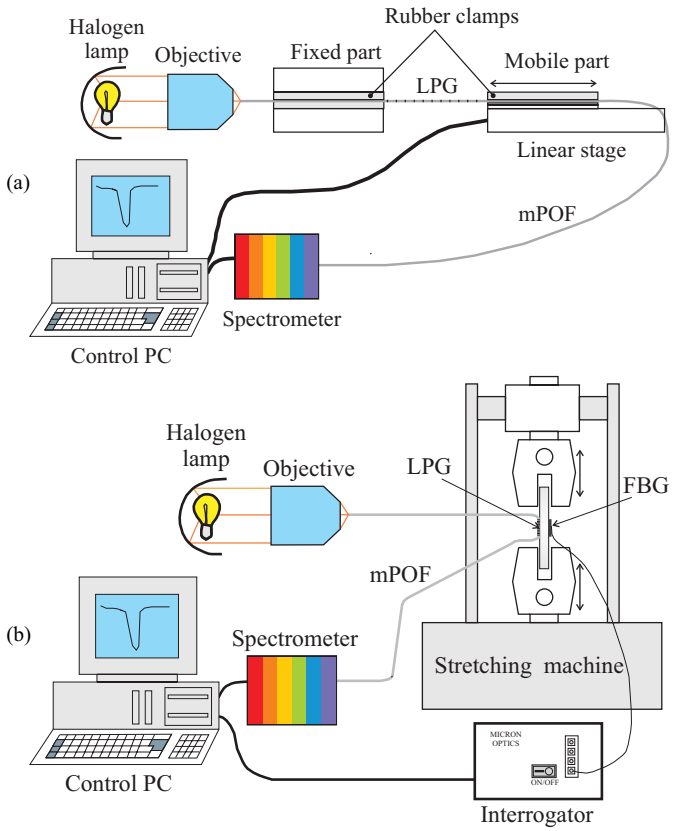

Fig. 3. Experimental setup for (a) optomechanical response of the LPG and (b) quasi-static loading of the proof specimen.

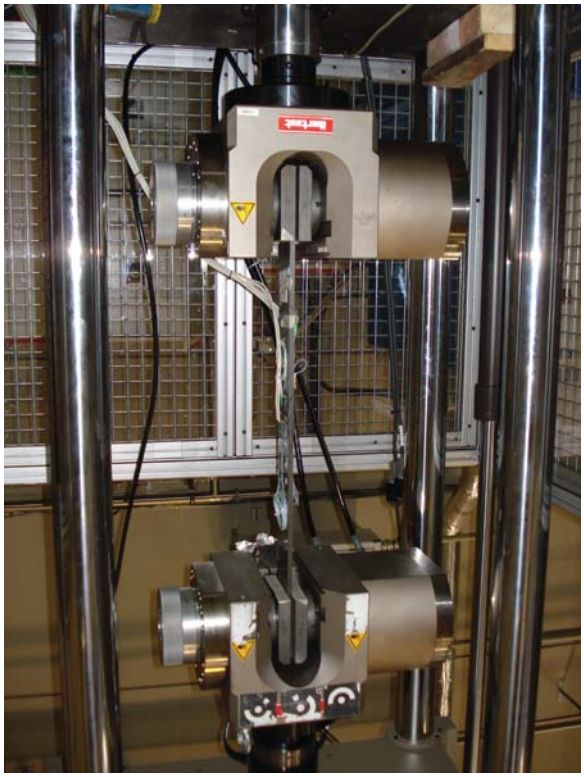

Fig. 4. Traction–compression machine used in the low cycle loading of the proof specimen.

used in the second scenario was located at a wavelength of 620 nm (without any applied strain) and the overall mPOF length was of 3 m. It is worthy of mention that the resonant wavelength did not coincide with the value provided by the manufacturer so that it evidenced the influence of the bonding material on the state of stress of the LPG, and consequently on its resonant wavelength. Regarding the non-coincidence between the loss feature wavelengths used in the first and second scenarios, there is no special reason for doing that; the different values are the result of the manufacturing process of the LPGs which does not have full control over the exact position of the resonant wavelength.

B. Experimental Programme

1) Instrumentation: As already explained in Sec. II-A (first scenario), these experiments were carried out on an LPG without embedding it in any bonding material. In order to evaluate the functionality of the mPOF sensor, different tests consisting of ramp-like and cyclical movements of the linear stage were carried out.

Regarding the experimental set-up used in these tests, white light from a halogen light bulb was launched into the fiber by means of a 20× microscope objective. The output spectrum was monitored using the USB4000 miniature fiber optic spectrometer from Ocean Optics with an spectral resolution of 1.28 nm at 550 nm. The tests were completely automated: a custom-built LabVIEW program controlled the precise movement of the linear stage and the wavelength of the loss feature was determined from the output spectrum of the LPG mPOF. A schematic drawing of the experimental set-up is shown in Fig. 3(a).

2) Quasi-Static Loading of the Proof Specimen: Several quasi-static loading tests (at frequencies of 0.2 Hz and 0.05 Hz) were conducted on the surface-bonded LPG to evaluate the response of the sensor and compare it with that of the FBG acting as a reference sensor (the latter being attached to the opposite surface of the plate). Additionally, these tests also served to compare the response of the surface-bonded LPG with that of the bare LPG (used in the first scenario). In this second scenario the plate was subjected to sinus- and ramp-tensile loadings by means of a traction/compression machine MTS 810 servo-hydraulic equipment which was able to apply scheduled stresses or strains through four hydraulic actuators at a maximum force of 500 kN. A picture of the machine installed at CTA facilities is shown in Fig. 4.

With respect to the experimental set-up, both the launching and the spectra acquisition systems were the same as those used in the first scenario. The loading programme applied to the proof specimen was controlled by means of proprietary software, and a custom-built LabVIEW program recorded the time response of the LPG, namely the shift in the wavelength of the loss feature due to the applied strain as a function of time. The data acquisition was made at a sampling frequency of 10/3 Hz (1 sample every 300 ms), which was sufficient for the different type of quasi-static loadings applied to the proof specimen. On the other hand, the response of the FBG used as a reference sensor was measured with the SM130-200 optical

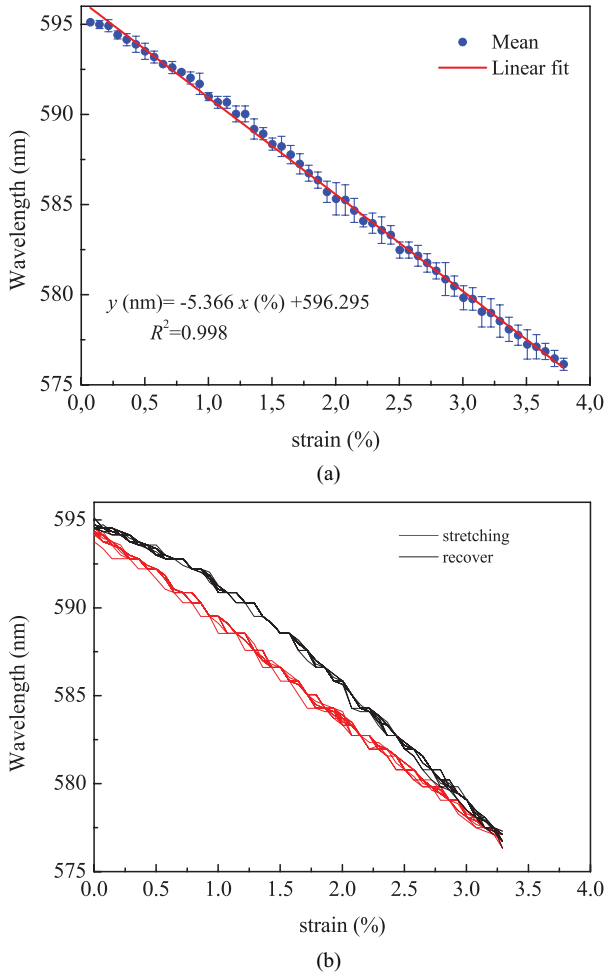

Fig. 5. Typical experimental results obtained in the first scenario. In both cases, the relationship between strain and the wavelength of the loss feature is shown. (a) Typical response of the sensor to the ramp-like loading of the LPG mPOF. Step size: 37.5 μm (0.07). (b) Typical response of the sensor to the ramp-like cyclical loading of the LPG mPOF. Number of repetitions: 15. Step size: 37.5 μm (0.07).

sensing interrogator from MicronOptics. In this case, the data adquisition (reflected wavelength as a function of time) was made at a sampling rate of 100 Hz (1 sample every 10 ms). The experimental set-up of this second scenario is shown in Fig. 3(b).

The strain, defined as the ratio of elongation $(L' - L)$ to the original length (L), has been determined from the measurement of L' and L. In the case of the first scenario, L' is the distance between clamps when the LPG is stretched, and L the distance between clamps when the LPG is not stretched but taut (reference position, $\epsilon = 0$). On the other hand, in the case of the second scenario, L' is the length of the proof specimen when the actuators are applying traction force to it, whereas L is the original length of the proof specimen ($L = 1$ m).

III. Results and Discussion

Figures 5(a) and 5(b) show typical results obtained in the first scenario for ramp-like and cyclical movements. In both cases the maximum applied strain was of 4 % with a step size of the linear stage of 37.5 μm (0.07 %).

In the first case (ramp-like loading, Fig. 5(a)) the measurements were repeated three times, and the mean value and its least mean squared curve-fit were calculated. It is clear from the mean value (blue dotted curve) that the sensor exhibits a high degree of strain linearity, a fact assessed by the very close to unity value of the R^2 coefficient derived from the fitting process (which is indeed $R^2 = 0.998$). This best fit is represented by the red line superimposed onto the blue dotted curve. However, for small strain values between 0 and 0.2 % a non-linear behavior can be observed. This may be attributed to the elastic properties of the rubber used to hold the LPG, which absorbed part of the stress applied by the linear stage and stored it in the form of strain energy.

In the context of this first scenario, a series of cyclical loading tests were also carried out to assess the repeatability of the response of the LPG mPOF sensor. Figure 5(b) shows a typical response over fifteen triangular-like loading cycles. The red curves correspond to the first half of the cycle where the LPG stretches from 0 % to 4 % strain, whereas the black curves correspond to the second half of the cycle, where the LPG recovers back to its starting position (0 % strain). First of all, it is worthy of mention that the reference position (0 % strain) has been redefined so that the initial non-linear response of the LPG mPOF has been removed. It can be clearly observed that, if each half-cycle is considered separately, there is a high degree of overlapping of the data points, thus ensuring a high repeatability in the response of the sensor. The asymmetric response between both half-cycles, with a curve-shape reminiscence of hysteresis, is mainly related to the characteristic elastic hysteresis of rubber, which in one sense makes the rubber harder to stretch when it is being loaded than when it is being unloaded [29]. Additionally, the recovery behavior of the fibers after each decrease of strain and the subsequent relaxation processes occurring in the polymer contribute to the hysteresis curve to a lesser extend [21].

It is also worth mentioning that the strain sensitivity of the sensor, obtained from the slope of any of the curves shown in Fig. 5, is limited by the LPG itself and not by the resolution of the spectrometer. Therefore, even though it is possible to decrease the uncertainty in the measurements of the sensor using the same LPG but an improved interrogation system, we can still make use of the present sensor configuration in a large number of applications where structural integrity represents an attractive avenue. In our measurements, the strain sensitivity of the bare sensor turned out to be of approximately 5.40 nm per elongation unit (expressed in %) or 0.54 pm/$\mu\epsilon$ (compare with the 1.48 pm/$\mu\epsilon$ for the PMMA FBG and to the 1.15 pm/$\mu\epsilon$ for the silica FBG) [16].

Figure 6 shows typical results obtained in the second scenario for a triangular-like tension cycling. The upper curve corresponds to the response of the LPG mPOF sensor and the lower curve to the response of the FBG reference sensor. First of all, we can observe that the raw signals provided by both sensors are out of phase 180° (that is, when the upper curve is maximum the lower one is minimum and vice versa). The reason for this lies in the opposite polarity of the slope $d\lambda/d\epsilon$ between the LPG mPOF used in the tests and silica-based FBGs ($d\lambda/d\epsilon < 0$ for LPGs in contrast to $d\lambda/d\epsilon > 0$ in silica-

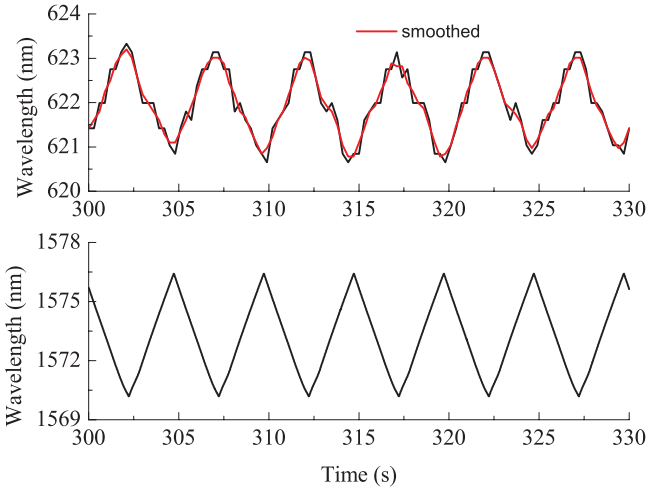

Fig. 6. Responses of the surface-bonded LPG mPOF (upper curve) and the surface-bonded FBG used as a reference sensor (lower curve) during a quasi-static triangular-like loading program of the proof specimen. Maximum strain applied: 0.5 %. Traction frequency: 0.2 Hz (1 cycle every 5 s).

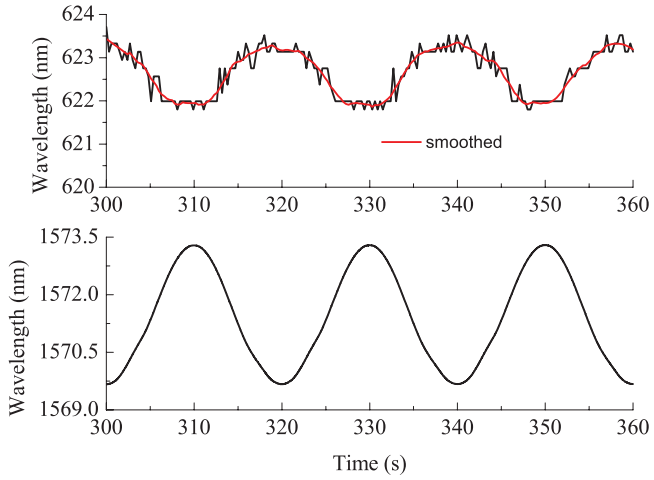

Fig. 7. Responses of the surface-bonded LPG mPOF (upper curve) and the surface-bonded FBG used as a reference sensor (lower curve) during a quasi-static sinus-like loading program of the proof specimen. Maximum strain applied: 0.3 %. Traction frequency: 0.05 Hz (1 cycle every 20 s).

based FBGs). In the case of the LPG mPOF sensor, the curve starts at a minimum of approximately 621 nm (corresponding to the maximum strain of 0.5 % applied to the plate by the stretching machine), and ramps up linearly to a maximum value of approximately 623.5 nm (corresponding to the strain-free position, 0 % strain, of the plate). It is also worthy of mention that this linear behavior between the strain values of 0 % and 0.5 % is not observed in the first scenario (see Fig. 5), where a rather poor response dominates. The reason for this is founded on the shift experienced by the resonant wavelength of the LPG used in the second scenario due to the bonding material. The response to strain now becomes linear, and consequently the cyclical loading applied to the plate modulates the resonant wavelength linearly, as shown in the upper curve of Fig. 6. The fluctuations observed are due to the limited resolution of the spectrometer which, according to the manufacturer, amounts to 1.28 nm at 550 nm. Additionally, it can also be observed that there are small differences in the wavelength values obtained at both extremes (minima and maxima), which is attributable to the fact that the data acquisition sampling frequency and the traction frequency are not related by an integer (10/3 Hz vs 0.2 or 0.05 Hz). Both artefacts can be partially overcome by filtering conveniently the curve. Although there exist many filtering schemes, a simple and efficient approach to filtering such a response is smoothing using nearest neighbours. The result of doing so is the red solid line shown in the upper curve of Fig. 6. None the less, and in spite of those inconveniences, it still can be concluded that the LPG mPOF sensor shows an excellent behavior for monitoring the strain level of the proof specimen.

The plate was also subjected to a sinus-like loading to assess the repeatability of the optical response under different loading conditions. In this case the maximum strain value applied was of 0.3 %. The typical response during three loading cycles is shown in Fig. 7. The upper curve corresponds to the LPG mPOF sensor and the lower curve to the FBG reference sensor. First of all, it is worth mentioning that, in the same way as in the triangular-like loading of the plate, both responses are out of phase 180°. As to the fluctuations shown by the response of the LPG mPOF sensor, these are more noticeable than those observed in the triangular-like loading of the plate (upper curve in Fig. 6). The reason for this lies again in the limited resolution of the spectrometer that has a stronger effect on the response of the sensor at those time intervals where the strain gradient is smaller. This way, these sinus-like curves are more affected than the previous triangular-like ones.

IV. Conclusion

In this paper, we have assessed the feasibility of using mechanically imprinted LPGs in single-mode mPOFs for strain sensing. A series of quasi-static loading tests consisting of ramp-like and cyclical movements were applied to a steel proof specimen in order to evaluate the performance of the surface-bonded LPG mPOF and compare it with the response of an FBG used as a reference sensor. The results show clearly the high sensitivity and elastic limit of the LPG mPOF sensor, exhibiting a high degree of signal repeatability and linearity as well. The oscillations of the optical response of the LPG mPOF, which account for the uncertainty, are due to the limited resolution of the spectrometer. Therefore, these test results do not impose any fundamental limitation to the resolution of the LPG itself. The preliminary results of the surface-bonded LPG mPOFs on a steel plate show encouraging results towards its implementation in SHM applications. Nevertheless, additional studies will be required to further characterize the functionality of the sensor and assess its suitability as an embedded sensor in a variety of structures.

References

[1] J. M. López-Higuera, Ed., *Handbook of Optical Fibre Sensing Technology*. New York: Wiley, 2002.
[2] K. Peters, "Polymer optical fiber sensors—a review," *Smart Mater. Struct.*, vol. 20, no. 1, pp. 013002-1–013002-17, 2011.
[3] B. Glišić and D. Inaudi, *Fibre Optic Methods for Structural Health Monitoring*. New York: Wiley, 2007.
[4] M. Luber, H. Poisel, S. Loquai, C. Neuner, A. Bachmann, O. Ziemann, and E. Hartl, "POF strain sensor using phase measurement techniques," in *Proc. Int. Cooperat. Plastic Opt. Fibers*, Sep. 2007, pp. 29–32.

[5] G. Durana, M. Kirchhof, M. Luber, I. S. de Ocáriz, H. Poisel, J. Zubia, and C. Vázquez, "Use of a novel fiber optical strain sensor for monitoring the vertical deflection of an aircraft flap," *IEEE Sensors J.*, vol. 9, no. 10, pp. 1219–1225, Oct. 2009.

[6] S. M. Melle, K. Liu, and R. M. Measures, "Strain sensing using a fiber-optic Bragg grating," *Proc. SPIE*, vol. 1588, pp. 255–263, Sep. 1991, doi: 10.1117/12.50184.

[7] K. S. C. Kuang, R. Kenny, M. Whelan, W. J. Cantwell, and P. R. Chalker, "Residual strain measurement and impact response of optical fibre Bragg grating sensors in fibre metal laminates," *Smart Mater. Struct.*, vol. 10, no. 2, pp. 338–346, 2001.

[8] K. S. C. Kuang and W. J. Cantwell, "The use of conventional optical fibres and fibre Bragg gratings for damage detection in advanced composite structures—a review," *Appl. Mech. Rev.*, vol. 56, no. 5, pp. 493–513, Sep. 2003.

[9] K. S. C. Kuang, S. T. Quek, C. G. Koh, W. J. Cantwell, and P. J. Scully, "Plastic optical fibre sensors for structural health monitoring: A review of recent progress," *J. Sensors*, vol. 2009, pp. 312053-1–312053-13, Jul. 2009, doi: 10.1155/2009/312053.

[10] K. S. C. Kuang and W. J. Cantwell, "The use of plastic optical fibre sensors for monitoring the dynamic response of fibre composite beams," *Meas. Sci. Technol.*, vol. 14, no. 6, pp. 736–745, 2003.

[11] H. Dobb, D. J. Webb, K. Kalli, A. Argyros, M. C. Large, and M. A. van Eijkelenborg, "Continuous wave ultraviolet light-induced fibre Bragg gratings in few-and single-moded microstructured polymer optical fibres," *Opt. Lett.*, vol. 30, no. 24, pp. 3296–3298, 2005.

[12] H. Y. Liu, H. B. Liu, G. D. Peng, and P. L. Chu, "Observation of type I and type II gratings behavior in polymer optical fiber," *Opt. Commun.*, vol. 220, nos. 4–6, pp. 337–343, May 2003.

[13] H. B. Liu, H. Y. Liu, G. D. Peng, and P. L. Chu, "Novel growth behaviors of fiber Bragg gratings in polymer optical fiber under UV irradiation with low power," *IEEE Photon. Technol. Lett.*, vol. 16, no. 1, pp. 159–161, Jan. 2004.

[14] P. J. Scully, D. Jones, and D. A. Jaroszynsky, "Femtosecond laser irradiation of polymethylmethacrylate for refractive index gratings," *J. Opt. A, Pure Appl. Opt.*, vol. 5, no. 4, pp. S92–S96, Jul. 2003.

[15] Z. Li, H. Y. Tam, L. Xu, and Q. Zhang, "Fabrication of long-period gratings in poly(methyl methacrylate-co-methyl vinyl ketone-co-benzyl methacrylate)-core polymer optical fiber by use of a mercury lamp," *Opt. Lett.*, vol. 30, no. 10, pp. 1117–1119, 2005.

[16] H.-B. Liu, H.-Y. Liu, G.-D. Peng, and P.-L. Chu, "Strain and temperature sensor using a combination of polymer and silica fibre Bragg gratings," *Opt. Commun.*, vol. 219, nos. 1–6, pp. 139–142, 2003.

[17] C. Zhang, W. Zhang, D.-J. Webb, and G.-D. Peng, "Optical fibre temperature and humidity sensor," *Electron. Lett.*, vol. 46, no. 9, pp. 643–644, Apr. 2010.

[18] M. C. J. Large, L. Poladian, G. W. Barton, and M. A. van Eijkelenborg, *Microstructured Polymer Optical Fibres*. New York: Springer-Verlag, 2007.

[19] M. A. van Eijkelenborg, M. Large, A. Argyros, J. Zagari, S. Manos, N. Issa, I. Basset, S. Fleming, R. McPhedran, C. M. de Sterke, and N. A. Nicorovici, "Microstructured polymer optical fibre," *Opt. Exp.*, vol. 9, no. 7, pp. 319–327, 2001.

[20] M. P. Hiscocks, M. A. van Eijkelenborg, A. Argyros, and M. C. J. Large, "Stable imprinting of long-period gratings in microstructured polymer optical fibre," *Opt. Exp.*, vol. 14, no. 11, pp. 4644–4649, 2006.

[21] M. C. J. Large, J. Moran, and L. Ye, "The role of viscoelastic properties in strain testing using microstructured polymer optical fibres (mPOF)," *Meas. Sci. Technol.*, vol. 20, no. 3, pp. 034014-1–034014-6, 2009.

[22] M. Steffen, M. Schukar, J. Witt, K. Krebber, M. Large, and A. Argyros, "Investigation of mPOF-LPGs for sensing applications," in *Proc. 18th Int. Conf. Plastic Opt. Fibers*, Sep. 2009.

[23] R. de Oliveira, M. Schukar, K. Krebber, and V. Michaud, "Advanced composite materials with embedded POF sensors for structural health monitoring," in *Proc. Int. Cooperat. Plastic Opt. Fibers*, Oct. 2010, p. 25.

[24] J. Witt, M. Steffen, M. Schukar, and K. Krebber, "Investigation of sensing properties of microstructured polymer optical fibres," *Proc. SPIE (Photon. Crystal Fibers IV)*, vol. 7714, p. 77140F, Apr. 2010.

[25] M. A. van Eijkelenborg, W. Padden, and J. A. Besley, "Mechanically induced long-period grating in microstructured polymer fibre," *Opt. Commun.*, vol. 236, nos. 1–3, pp. 75–78, Jun. 2004.

[26] S. Savin, M. J. F. Digonnet, G. S. Kino, and H. J. Shaw, "Tunable mechanically induced long-period fiber gratings," *Opt. Lett.*, vol. 25, no. 10, pp. 710–712, 2000.

[27] V. Bhatia, "Properties and sensing applications of long-period gratings," Ph.D. dissertation, Dept. Electr. Eng., Virginia Tech, Blacksburg, 1996.

[28] K. O. Hill and G. Meltz, "Fiber Bragg grating technology fundamentals and overview," *J. Lightw. Technol.*, vol. 15, no. 8, pp. 1263–1276, Aug. 1997.

[29] N. G. McCrum, C. P. Buckley, and C. B. Bucknall, *Principles of Polymer Engineering*. London, U.K.: Oxford Univ. Press, 1997.

Gaizka Durana received the B.Sc. degree in solid-state physics and the Ph.D. degree in engineering from the University of the Basque Country, Bilbao, Spain, in 1999 and 2008, respectively. His Ph.D. work focused on the experimental and numerical analysis of fundamental aspects of light propagation in multimode optical fibers.

His current research interests include manufacture of photonic crystal fibers and their application in sensing.

Dr. Durana received a European acknowledgement of his Ph.D. degree Doctor Europeus in 2008.

Javier Gómez received the M.Sc. degree in telecommunications engineering from the University of the Basque Country, Bilbao, Spain, in 2006. He is currently pursuing the Ph.D. degree with the Applied Photonics Group, University of the Basque Country, Bilbao, Spain.

Gotzon Aldabaldetreku received the M.Sc. and Ph.D. degrees in telecommunications engineering from the University of the Basque Country, Bilbao, Spain, in 2000 and 2006, respectively. His Ph.D. work focused on the theoretical analysis of light propagation properties in multimode multistep index optical fibers.

He is currently an Assistant Professor with the Department of Electronics and Telecommunications, School of Engineering of Bilbao, University of the Basque Country. He has more than ten years of experience in basic research in the field of polymer optical fibers, and is currently involved in research projects in the field of characterization and fabrication of polymer optical fibers and fiber-optic sensors. He was involved in international research projects with other universities and companies.

Dr. Aldabaldetreku was a recipient of a European acknowledgement of the Ph.D. degree.

Joseba Zubia received the M.Sc. degree in solid-state physics and the Ph.D. degree in physics from the University of the Basque Country, Bilbao, Spain, in 1988 and 1993, respectively. His Ph.D. work focused on the optical properties of ferro electric liquid crystals.

He is currently a Full Professor with the Department of Electronics and Telecommunications, School of Engineering of Bilbao, University of the Basque Country. He has more than 12 years of experience in basic research in the field of polymer optical fibers, and is currently involved in research projects in collaboration with universities and companies from Spain and other countries in the field of polymer optical fibers, fiber-optic sensors, and liquid crystals.

Dr. Zubia was a recipient of a Special Award for Best Thesis in 1995.

Ander Montero received the B.Sc. degree in aeronautical engineering from the Polytecnic University of Madrid, Madrid, Spain, in 2008.

He is currently a Project Manager of avionics research projects at the singular program area, Aeronautical Technological Center, Vitoria, Spain.

Idurre Sáez de Ocáriz received the M.Sc. degree in solid-state physics and the Ph.D. degree in physics from the University of the Basque Country, Bilbao, Spain, in 1995 and 2001, respectively. Her Ph.D. work focused on the optical properties (laser spectroscopy) of Pr3+ in crystals and glasses. She also received the Postgraduate degree in management and organization of research and innovation from the Polytechnic University of Madrid, Madrid, Spain, in 2005.

She is currently the Head of research and development with the Aeronautical Technological Center, Vitoria, Spain.